THE JOURNAL OF PHYSICAL CHEMISTRY B LETTERS

2006, *110,* 25568−25572
Published on Web 11/30/2006

Size-Dependent Spectroscopic Properties of Conjugated Polymer Nanoparticles

John K. Grey, Doo Young Kim, Brent C. Norris, William L. Miller, and Paul F. Barbara*

Center for Nano- and Molecular Science and Technology and Department of Chemistry and Biochemistry, University of Texas at Austin, Austin, Texas 78712

Received: September 13, 2006; In Final Form: November 10, 2006

This paper is focused on how the spectroscopic properties of conjugated polymers evolve in the size range between single polymer chains and the bulk material. The measurements used single-particle spectroscopy techniques and include both static and dynamic measurements. The main observation of this work is that the spectroscopic properties of MEH-PPV evolve rapidly as a function of nanoparticle size and achieve bulk-like properties for nanoparticles greater than 10 nm in size. Nanoparticles were assembled by a reprecipitation technique and characterized by fluorescence emission spectroscopy. The physical origin of the size-dependent spectroscopic properties is assigned to the distance dependence of four main processes: electronic energy transfer between blue and red sites, triplet−triplet annihilation, singlet exciton quenching by triplets, and singlet exciton quenching by hole polarons.

Introduction

The spectroscopy of conjugated polymers has been investigated intensely for decades. With the advent of new size-dependent and spatially resolved spectroscopic methods, there has been a growing appreciation that these functional materials (e.g., for OLEDs and photovoltaic cells) are highly spatially heterogeneous because of morphological effects, such as chain−chain packing,[1] conformational defects and distortions of the polymer chain,[2−5] aggregation,[1,6−10] and so forth. It is now clear that the emission of bulk conjugated polymer thin films (i.e., the functional form of conjugated polymers) is due primarily to singlet excitons that are trapped in dilute, low-energy "red sites" that are spatially distributed in the polymer film.[6] The red sites are apparently due to local well-packed regions on the polymer chain that have relatively close chain−chain contacts. The energy lowering at red sites has been ascribed alternatively to chain−chain electronic interactions or alternatively to an increase in the conjugation length due to a more tightly folded polymer chain. The absorption, however, occurs predominately to more plentiful "blue sites", which in many cases correspond to more than 95% of the polymer segments. It has been shown, furthermore, that the efficiency of energy transfer from the blue sites to the red sites can approach unity for the bulk polymer film, even at cryogenic temperatures.[11]

Interestingly, energy transfer from blue to red sites can be significantly suppressed in isolated single polymer chains, apparently because of the small number of red sites per chain. Typically, single polymer chains have been investigated with molecular weights in the range of 10^4-10^6 amu, that is, corresponding to molecular radii of the collapsed polymer chain in the range of 4−8 nm, respectively. Fluorescence single-molecule spectroscopy (SMS) of isolated polymer chains has led to detailed information on the energy distribution of local electronic excited states in a single polymer chain.[12−21]

Recent intensive SMS and bulk film spectroscopic studies on the prototypical conjugated polymer MEH-PPV have shown unequivocally that emitting-state energy distributions are bimodal, corresponding to emission from two distinct (i.e., blue and red) species.[2,13,22,23] The energy splitting between emission maxima of the blue and red forms is ∼0.1 eV,[13,22,23] and the relative amounts of each form has also been shown to be molecular-weight-dependent.[24] Therefore, SMS of conjugated polymers provides a unique window on the effect of morphology on the spectroscopy of conjugated polymers with regard to the role of red sites, especially at cryogenic temperatures where the spectra are well-resolved.[18,19,24,25] In addition, time-resolved SMS methods have led to detailed information on the *spectroscopic dynamics* of conjugated polymers. This includes dynamical measurements on triplet excitons,[26,27] singlet excitons,[12,13] and polarons (charges).[28−30] Indeed, a clear picture of how the heterogeneity of conjugated polymers influences the interaction of excitons and polarons on the nanoscale is beginning to emerge.

This paper is focused on a detailed investigation of how the spectroscopic properties of nanoparticles assembled from conjugated polymer chains evolve in the size range between single polymer chains and the bulk material. This was achieved by investigating the spectroscopy of assembled nanoparticle aggregates of conjugated polymer chains as a function of size, in the approximate range of ∼10−100 nm in radius. The measurements used single-particle spectroscopy techniques, including both static and dynamic measurements and measured the effect of particle size on the frequency-resolved photoluminescence spectra of conjugated polymers, the photobleaching dynamics, and triplet−triplet annihilation kinetics.

Experimental Section

MEH-PPV nanoparticles were prepared by a reprecipitation method adapted from the literature.[31] MEH-PPV (MW =

* Corresponding author. E-mail: p.barbara@mail.utexas.edu.

10.1021/jp065990a CCC: $33.50

186 000 amu) was obtained as a gift from the Ferraris group (University of Texas, Dallas) and was dissolved in THF (Aldrich) at a concentration of $\sim 10^{-6}$ M. Two milliliters of THF solution was added rapidly to 8 mL of deionized water (15 MΩ) while simultaneously sonicating the solution. MEH-PPV is not soluble in water, and precipitation of nanoparticles occurs rapidly when the THF solution is added to the water. Sonication was continued for an additional 30 min after the addition was complete. The solution was then heated in a warm water bath to evaporate the THF. The resultant solution was filtered using a 0.1 μm syringe filter (Whatman) yielding a nanoparticle stock solution of particles with the size distribution described below. The size distribution and spectroscopy of the particles of the stock solution was stable for several weeks. Variable MW samples used for SMS studies were prepared according to ref 24.

Nanoparticle samples in thin films (100 nm) of polyvinyl alcohol (PVA, Aldrich) were prepared by spin-coating an aqueous solution of PVA (4%) containing a small aliquot of a freshly prepared nanoparticle stock solution onto a rigorously cleaned microscope cover-slip. Subsequent to spin-coating, the samples were exposed to vacuum for an extended period to remove water and oxygen, followed by evaporation of a gold over-layer to seal the sample and maintain a low concentration of oxygen in the thin film.

The SMS data was acquired using a standard confocal microscope/spectrometer approach. Two different previously described instruments were used, respectively, for the ambient temperature[13,14] and low temperature[24] SMS measurements. A 488 nm Ar ion laser line was used to excite the nanoparticles. Polarization modulation experiments were accomplished using an electro-optical modulator operating at a frequency of 1 kHz and intensity modulation measurements used acoustic-optical modulators with synchronously averaged detection.

Results and Discussion

Figure 1A shows a confocal fluorescence image of an ensemble of assembled nanoparticles of MEH-PPV dissolved in a 100-nm-thick PVA film. The isolated fluorescence spots in the image are due to the individual nanoparticles. Under low intensity ($\sim$4 W/cm^2) irradiation conditions, the spot intensities in the confocal images are highly reproducible with very little evidence of photobleaching, intensity saturation due to the build up of triplets, or photochemistry. The line scans of the individual spots in the confocal images of the nanoparticles reveal a diffraction-limited spot size (fwhm) of $\sim$300 nm that is indistinguishable from the spot size of small single molecules on our apparatus, demonstrating that the nanoparticles are $\ll$300 nm in diameter.

On the basis of an assumption of constant quantum yield and constant absorption cross section per polymer spectroscopic unit, the spot intensity can be used as an approximate, linear measure of the "particle weight" (PW). The mean fluorescence intensity of an ensemble of isolated single polymer chains with a mean MW of 186 000 amu imaged under the same conditions as the nanoparticle samples was used as a secondary standard leading to the calibration in the bottom axis of the particle intensity histogram shown in Figure 1B. The size of individual nanoparticles can then be roughly estimated from the particle weight by assuming a spherical shape of the nanoparticles, and a density of 0.8 g/mL, resulting in a rough calibration for the particle radius, r_P. From the above assumptions, we estimate an r_P of $\sim$20 nm for the nanoparticles, which is in good agreement with the lower size limit established from AFM measurements.

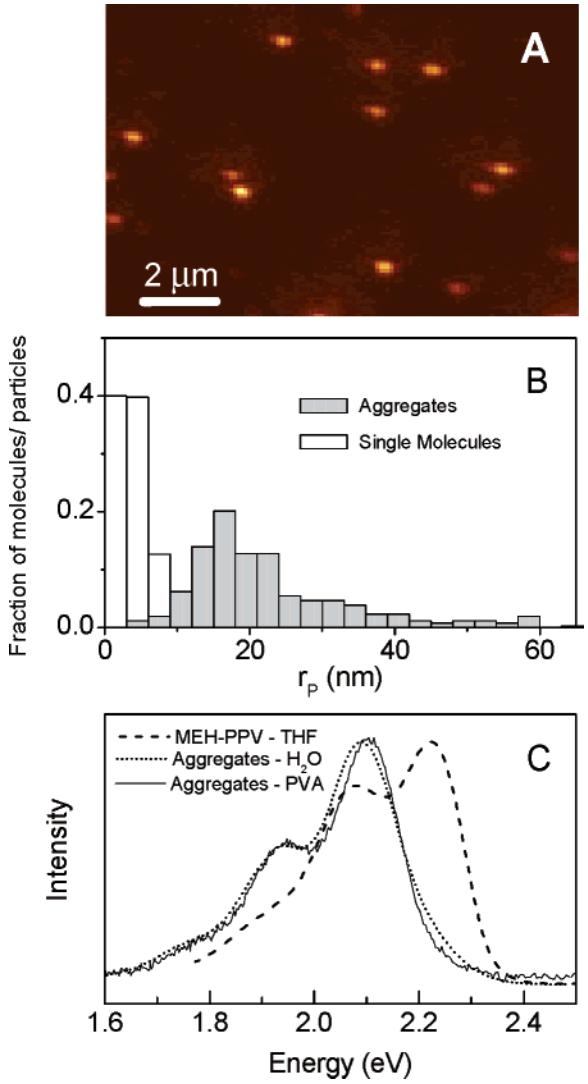

Figure 1. (A) Fluorescence image of single nanoparticles of MEH-PPV diluted in a PVA matrix obtained with 488 nm excitation (50 W/cm^2). (B) Estimated size distributions (particle radii, r_P) from $\sim$200 MEH-PPV single molecules and nanoparticles. (C) Fluorescence emission spectra of MEH-PPV nanoparticles in dilute PVA thin films (solid line), aqueous suspension (dotted line), and in THF (dashed line) measured at 298 K. The dilute film spectrum is obtained by summing $\sim$75 single nanoparticle aggregate spectra.

Frequency-Resolved Fluorescence Spectra. The emission spectra of an ensemble of nanoparticles at ambient temperature was observed to be insensitive to environment, (e.g., water vs PVA), suggesting that the emission is dominated by the core of the nanoparticles, not the surface. In fact, the assembled nanoparticle samples have an emission spectrum that is very close to bulk thin-film MEH-PPV samples (dashed line in Figure 2F). The nanoparticle spectra are significantly red-shifted from MEH-PPV dissolved in THF (Figure 1C), a good solvent for MEH-PPV. This is consistent with expectations that in a good solvent the polymer conformation should be extended without chain−chain contacts, and as a result, lack low-energy sites for singlet excitons.[15,23,32]

The effect of particle size on the frequency-resolved emission spectra is especially apparent in low temperature (20 K) SMS data, as shown in Figure 2. Figure 2B, D, and F reveal the evolution of the ensemble spectra as the particle size is increased. Figure 2B and D are ensemble spectra of single polymer chains with molecular weights of 186 000 and 1 000 000 amu, respectively. These data reveal the previously described

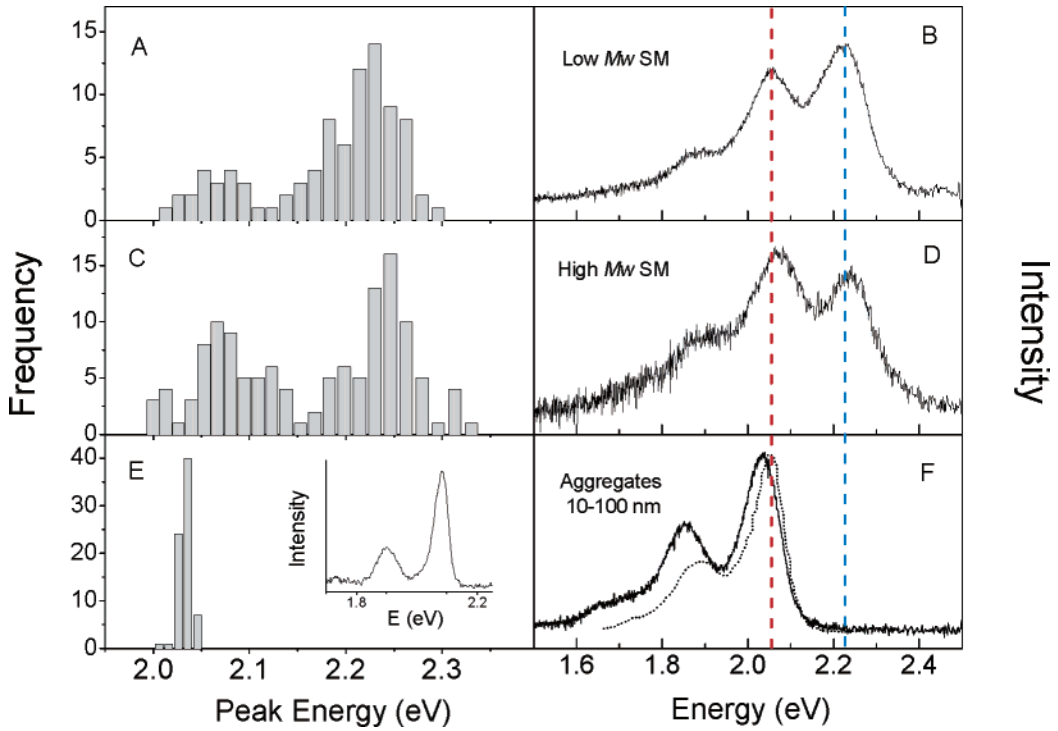

Figure 2. Peak wavelength histograms and ensemble emission spectra of MEH-PPV single molecules (SM) and nanoparticle aggregates measured at 20 K. (A and B) 186 kDa; (C and D) 1000 kDa; (E and F) aggregates. A bulk film MEH-PPV emission spectrum measured at 4 K (dashed line) is shown for comparison and the inset in E shows a single nanoparticle spectrum measured at 20 K. The red and blue vertical dashed lines through B, D, and F denote red and blue peak energy maxima, respectively.

superposition of emission from high energy "blue" sites and low energy "red" sites[13] indicated by the vertical dashed blue and red lines in Figure 2. Absorption of 488 nm light excites the blue sites, some of which subsequently transfer energy to the red sites. This phenomenon has been described extensively in previous papers from our laboratory.[12−14,20,24,33,34]

Parts A and C of Figure 2 are histograms of the emission energy maxima of low- and high-MW single molecules whose ensemble spectra is shown in Figure 2B and D, respectively. The vibronic features in the ensemble spectra in Figure 2B and D are significantly broader than the individual single-molecule spectra that were used to construct the ensemble spectra. The broadening is due to molecule-to-molecule conformational and environmental variations. An example of an individual nanoparticle spectrum is shown in Figure 2E. Both SM histograms exhibit the previously reported characteristic "bimodal" distribution behavior[12,13] associated with blue and red sites. The red sites have been assigned previously (see Introduction) to dilute low-energy sites along the polymer chain that are excited primarily by energy transfer from the more plentiful blue sites. Clearly the ratio of blue to red emitting species changes with molecular weight (chain length).[24] The much higher probability of observing emission from the blue sites in the low MW samples is due to the relatively small size of these polymer chains and the presence of very few red sites per chain (in some cases none). For larger single-molecule chains shown in Figure 2C and D, there is a higher probability of a chain possessing a red site (i.e., increase in chain−chain contacts). As a result, the distribution of emission maxima (Figure 2C) has nearly equally probable blue-emitting molecules. Although the energy splitting between blue and red forms is close to the dominant progression interval, this feature is purely accidental and is not due to vibronic (false) origins or large emitting-state displacements (Huang−Rhys factors).[24]

Interestingly, assembling several polymer chains together has an enormous effect on the emission spectroscopy. The emission maxima histogram of nanoparticles (Figure 2E) collapses to a single peak close to the emission maxima of bulk MEH-PPV dominated by red sites. In addition, the ensemble emission spectrum of the assembled nanoparticles closely resembles the spectrum of the bulk thin film (Figure 2E, dashed line), which is in excellent agreement with previous observations in MEH-PPV aggregate systems.[8] A detailed investigation of different particles in the ensemble revealed that even the smaller assembled nanoparticles exhibit spectra that are dominated by red site emission. The fact that the core of the assembled nanoparticles are spectroscopically indistinguishable from the bulk thin film suggests that bulk-like structure and properties are achieved for MEH-PPV for particle radii greater than approximately 10 nm.

The complete absence of blue sites in the emission of the multichain-assembled nanoparticles strongly suggests that there is a large increase in both the number and concentration of red sites for this form of MEH-PPV. In addition, the extreme narrowing of the emission maxima histogram suggests the presence of a large concentration of red sites with a narrow distribution of emission energies. Apparently, the assembly process in multichain-assembled nanoparticles involves a cooperative formation of red sites, probably through *inter*-chain interactions. Previous publications have shown that annealing can dramatically increase the number of red sites in bulk polymers.[6,35−37] It may be that the assembly and growth methods associated with the precipitation method used herein in fact favor the formation of red sites.

It is interesting to compare the width of the peak in the emission maxima histogram for the assembled nanoparticles to the corresponding red site peak in the smaller single-molecule particles. The broader width in the latter case has been shown previously to be due to a weak component of blue site emission that tends to shift the emission maxima of the molecules with primarily red emission and conformational heterogeneity from molecule to molecule.[24] The narrow width of the peak for the

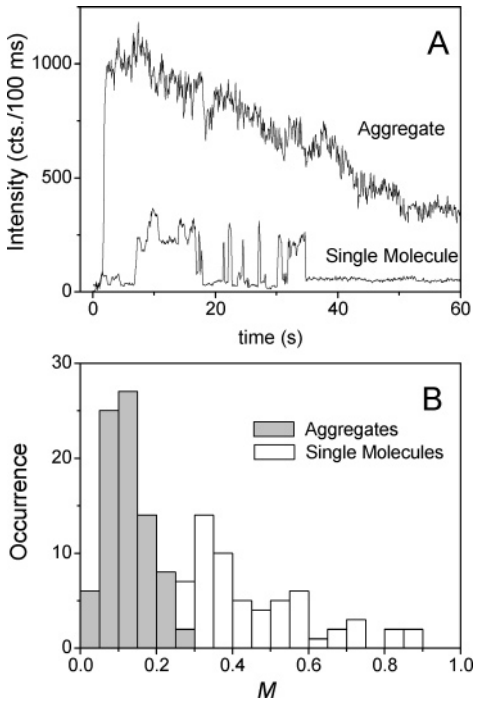

Figure 3. (A) Intensity transients of a MEH-PPV single aggregate nanoparticle and single MEH-PPV molecule. Excitation intensities were approximately 300 W/cm^2. (B) Polarization anisotropies of aggregate nanoparticles and MEH-PPV single molecules (186 000 amu).

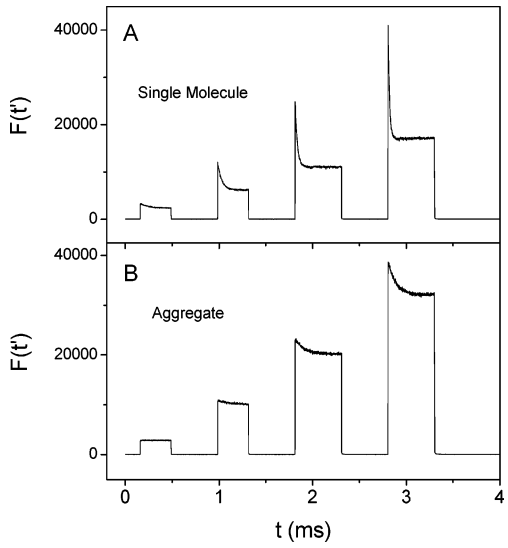

Figure 4. Representative intensity modulation transients of (A) MEH-PPV single molecules and (B) MEH-PPV nanoparticles excited with 488 nm light at 298 K. Excitation intensities of the four excitation pulses are 90, 350, 500, and 850 W/cm^2, respectively. A 0.5 OD neutral density filter was placed in the detection path for nanoparticle transient measurements to obtain comparable intensities to the single molecules.

assembled nanoparticles is further indication that essentially no detectable blue emission is present in these particles and also suggests that energy funneling among red sites may be operating, ensuring nearly identical emission maxima for all particles. Both of these observations are consistent with a large number of red sites per assembled nanoparticle capable of intra-site energy transfer.

Photobleaching Kinetics. The photobleaching kinetics of organic nanoparticles is compared to that for single conjugated polymer chains in Figure 3A using unsealed samples (i.e., without a metal overcoating). As reported previously, single polymer chains exhibit discrete florescence intensity "blinking" due to single photo-oxidation events, involving primarily photochemically injected positive charges.[13,38] The positive charges are apparently injected by an electron-transfer mechanism involving trapping by molecular oxygen.[13,28,29] A single positive charge (polaron) has been shown to be able to efficiently quench single excitons in conjugated polymers with a "quenching radius", r_Q, on the order of 5 nm.[39] For single conjugated polymer chains with a radius in this size range, single positive charges injected by photo-oxidation can, therefore, induce large changes in the emission intensity, and produce a blinking-like effect.

Interestingly, for the larger nanoparticles, the drop in fluorescence intensity due to photo-oxidation occurs less discretely than that observed with single molecules. A typical photobleaching curve is shown in Figure 3A. The individual intensity drops due to successive photobleaching events are only slightly larger than the noise in the transients due to shot noise. For a fresh particle, the initial blinking events are <7 % of the initial intensity. An order-of-magnitude estimate for the polaron-induced quenching depths, Q_D, for an assembled nanoparticle is given by the ratio of the exciton quenching volume to the volume of a particle, that is, $Q_D \sim (r_Q/r_P)^3 \sim 0.02$ (2%). This is the same order of magnitude as the experimental blinking depths for the assembled nanoparticles. In addition, the possibility of multiple sites for photo-oxidation, each with a different exciton capture radius, should be another factor that will tend to mask discrete intensity drops due to photobleaching in the assembled nanoparticles.

Polarization Spectroscopy. Figure 3B presents data on the optical excitation polarization anisotropy for MEH-PPV nanoparticles and single polymer chains, both imbedded in rigid polymer hosts. Because the $\pi-\pi^*$ transitions responsible for the absorption of MEH-PPV are polarized along the direction of the polymer backbone, the excitation polarization anisotropy is a measure of the degree of orientational anisotropy of the polymer chain(s) in a particle.[14,40] The polarization modulation parameter, M, was determined as described previously by rotating the polarization direction of a linearly polarized excitation beam, while synchronously recording the emission intensity with an unpolarized detection scheme. For each molecule (or nanoparticle), i, intensities are averaged over many cycles and fitted to

$$I \propto 1 + M \cos 2(\theta - \varphi) \qquad (1)$$

where I is the emission intensity as a function of the direction of polarization in the plane of the sample, Θ, of the excitation light, φ is the direction of preferred absorption for a particular molecule or particle, and $M = (I_{||} - I_{\perp})/(I_{||} + I_{\perp})$.

The M histogram for MEH-PPV single molecules (MW = 186 000 amu) in Figure 3B reveals a broad distribution of M values, consistent with previous measurements.[14,40] This type of distribution has been interpreted as being due to a parallel arrangement of chromophores in polymer chains due to a "cylindrical" polymer chain conformation.[14] Interestingly, the M histogram for the nanoparticles indicates that these species are much less ordered, with M values that are only slightly larger than experimental error (~0.05). This suggests that the nanoparticles have a sufficient number of polymer chains, arranged in a random direction such that there is little anisotropy on the particle radius scale. This is analogous to the situation in bulk MEH-PPV, and other conjugated polymers, where the emission anisotropy is small (<10%), even on the 100 nm size scale.[35]

Triplet−Triplet Annihilation and Singlet Quenching by Triplets. Another photodynamical effect for MEH-PPV that shows evidence of being size-dependent is the triplet−triplet

annihilation kinetics. Gesquiere et al. recently introduced a high signal-to-noise technique for studying triplet dynamics in multichromophoric molecules, namely, *single-molecule excitation intensity modulation spectroscopy*.[27] In this approach, the fluorescence intensity $F(t)$ of a single conjugated polymer molecule (or nanoparticle) is recorded while irradiating the molecule with many repetitive cycles of a sequence of submillisecond time scale excitation pulses. $F(t)$ is synchronously averaged over many cycles to yield time ensemble intensity $F(t')$ versus t' curves, where t' refers to time within the cycle. Representative $F(t')$ curves for MEH-PPV single molecules and assembled nanoparticles in the PVA samples are shown in Figure 4A and B, respectively. Samples were excited with 488 nm light with an average intensity of 300 W/cm^2. Because nanoparticles are considerably brighter than single molecules under the same excitation conditions, it was necessary to attenuate signals with neutral density filters (0.5 OD) in order to maintain comparable intensities.

The decrease in modulation depth with increasing particle size is apparently a reflection of an increased impact of triplet−triplet annihilation on the relative triplet population. Because triplet−triplet annihilation is a bimolecular process, it cannot occur for concentrations below one triplet per particle because a triplet cannot annihilate itself.[26,27,30] For small particles this can be an extremely important effect, leading to a very large average triplet population, even under moderate to low excitation intensities.[26,27,30] In this case, singlet quenching by triplets dominates, giving rise to the large modulation depths in Figure 4A. For large particles, emission is quenched much less because one triplet simply cannot efficiently quench the more plentiful singlet emitting sites (Figure 4B).

Conclusions and Summary

This work reports that the spectroscopic properties of conjugated polymer assembled nanoparticles evolve rapidly as a function of particle size and achieve bulk-like properties for nanoparticles greater than ∼10 nm in radius. The observed size-dependent spectroscopic properties are assigned to the distance dependence of four main kinetic processes, electronic energy transfer between blue and red sites, triplet−triplet annihilation, singlet exciton quenching by triplets, and singlet exciton quenching polarons. In addition, the spectroscopic data indicate that the assembled nanoparticles have a much higher concentration per volume of red sites than the single polymer chains. This latter effect may be a due to a size-dependent rate of forming red sites during assembly due to cooperativity in the assembly and growth process. It is interesting that the physical origin of the size-dependent properties of organic semiconductor nanoparticles are entirely different from those known to be operating for inorganic semiconductor nanoparticles, for which the spatial confinement of excitons is the dominant effect.

Acknowledgment. We gratefully acknowledge support of the National Science Foundation and the Welch Foundation for support of this research. JKG acknowledges the Petroleum Research Fund of the American Chemical Society for a fellowship.

References and Notes

(1) Peng, K.-Y.; Chen, S.-A.; Fann, W.-S.; Chen, S.-H.; Su, A.-C. *J. Phys. Chem. B* **2005**, *109*, 9368.
(2) Collison, C. J.; Rothberg, L. J.; Treemaneekarn, V.; Li, Y. *Macromolecules* **2001**, *34*, 2346.
(3) Wong, K. F.; Skaf, M. S.; Yang, C.-Y.; Rossky, P. J.; Bagchi, B.; Hu, D.; Yu, J.; Barbara, P. F. *J. Phys. Chem. B* **2001**, *105*, 6103.
(4) Grage, M. M. L.; Wood, P. W.; Ruseckas, A.; Pullerits, T.; Mitchell, W.; Burn, P. L.; Samuel, I. D. W.; Sundström, V. *J. Chem. Phys.* **2003**, *118*, 7644.
(5) Padmanaban, G.; Ramakrishnan, S. *J. Phys. Chem. B* **2004**, *108*, 14933.
(6) Schwartz, B. J. *Ann. Rev. Phys. Chem.* **2003**, *54*, 141.
(7) Blatchford, J. W.; Gustafson, T. L.; Epstein, A. J.; Vanden Bout, D. A.; Kerimo, J.; Higgins, D. A.; Barbara, P. F.; Fu, D.-K.; Swager, T. M.; MacDiarmid, A. G. *Phys. Rev. B* **1996**, *54*, R3863.
(8) Chang, R.; Hsu, J.-H.; Fann, W.-S.; Yu, J.; Lin, S.-H.; Lee, Y.-Z.; Chen, S.-A. *Chem. Phys. Lett.* **2000**, *317*, 153.
(9) Nguyen, T. Q.; Martini, I. B.; Liu, J.; Schwartz, B. J. *J. Phys. Chem. B* **2000**, *104*, 237.
(10) Collison, C. J.; Treemaneekarn, V.; Oldham, W. J.; Hsu, J.-H.; Rothberg, L. J. *Synth. Met.* **2001**, *119*, 515.
(11) Gaab, K. M.; Bardeen, C. J. *J. Phys. Chem. B* **2004**, *108*, 4619.
(12) Hu, D.; Yu, J.; Barbara, P. F. *J. Am. Chem. Soc.* **1999**, *121*, 6936.
(13) Yu, J.; Hu, D.; Barbara, P. F. *Science* **2000**, *289*, 1327.
(14) Hu, D.; Yu, J.; Wong, K.; Bagchi, B.; Rossky, P. J.; Barbara, P. F. *Nature* **2000**, *405*, 1030.
(15) Huser, T.; Yan, M.; Rothberg, L. J. *Proc. Natl. Acad. Sci.* **2000**, *97*, 11187.
(16) Wang, C. F.; White, J. D.; Lim, T. L.; Hsu, J.-H.; Yang, S.-C.; Fann, W.-S.; Peng, K.-Y.; Chen, S.-A. *Phys. Rev. B* **2003**, *67*, 035202:1.
(17) Rønne, C.; Trägårdh, J.; Hessman, D.; Sundström, V. *Chem. Phys. Lett.* **2004**, *388*, 40.
(18) Schindler, F.; Lupton, J. M. *ChemPhysChem* **2005**, *6*, 926.
(19) Becker, K.; Lupton, J. M. *J. Am. Chem. Soc.* **2005**, *127*, 7306.
(20) Barbara, P. F.; Gesquiere, A. J.; Park, S.-J.; Lee, Y.-J. *Acc. Chem. Res.* **2005**, *38*, 602.
(21) Sun, W.-Y.; Yang, S.-C.; White, J. D.; Hsu, J.-H.; Peng, K.-Y.; Chen, S.-A.; Fann, W.-S. *Macromolecules* **2005**, *38*, 2966.
(22) Wang, P.; Cuppoletti, C. M.; Rothberg, L. J. *Synth. Met.* **2003**, *137*, 1461.
(23) Wachsmann-Hogiu, S.; Peteanu, L. A.; Liu, L. A.; Yaron, D. J.; Wildeman, J. *J. Phys. Chem. B* **2003**, *107*, 5133.
(24) Kim, D. Y.; Grey, J. K.; Barbara, P. F. *Synth. Met.* **2006**, *156*, 336.
(25) Yu, Z.; Barbara, P. F. *J. Phys. Chem. B* **2004**, *108*, 11321.
(26) Yu, J.; Lammi, R.; Gesquiere, A. J.; Barbara, P. F. *J. Phys. Chem. B* **2005**, *109*, 10025.
(27) Gesquiere, A. J.; Lee, Y.-J.; Yu, J.; Barbara, P. F. *J. Phys. Chem. B* **2005**, *109*, 12366.
(28) Park, S.-J.; Gesquiere, A. J.; Yu, J.; Barbara, P. F. *J. Am. Chem. Soc* **2004**, *126*, 4116.
(29) Gesquiere, A. J.; Park, S.-J.; Barbara, P. F. *J. Phys. Chem. B* **2004**, *108*, 10301.
(30) Gesquiere, A. J.; Park, S.-J.; Barbara, P. F. *J. Am. Chem. Soc* **2005**, *127*, 9556.
(31) (a) Szymanski, C.; Wu, C.; Hooper, J.; Salazar, M. A.; Perdomo, A.; Dukes, A.; McNeill, J. D. *J. Phys. Chem. B* **2005**, *109*, 8543. (b) Wu, C.; Peng, H.; Jiang, Y.; McNeill, J. *J. Phys. Chem. B* **2006**, *110*, 14148.
(32) Zhang, H.; Lu, X.; Li, Y.; Ai, X.; Zhang, X.; Yang, G. *J. Photochem. Photobiol., A* **2002**, *147*, 15.
(33) Lammi, R. K.; Barbara, P. F. *Photochem. Photobiol. Sci.* **2005**, *4*, 95.
(34) Grey, J. K.; Kim, D. Y.; Lee, Y. J.; Gutierrez, J. J.; Luong, N.; Ferraris, J. P.; Barbara, P. F. *Angew. Chem. Int. Ed.* **2005**, *44*, 6207.
(35) Tan, C. H.; Inigo, A. R.; Hsu, J.-H.; Fann, W.; Wei, P.-K. *J. Phys. Chem. Solids* **2001**, *62*, 1643.
(36) Schaller, R. D.; Snee, P. T.; Johnson, J. C.; Lee, L. F.; Wilson, K. R.; Haber, L. H.; Saykally, R. J.; Nguyen, T. Q.; Schwartz, B. J. *J. Chem. Phys.* **2002**, *117*, 6688.
(37) Chen, S.-H.; Su, A.-C.; Han, S.-R.; Chen, S.-A.; Lee, Y.-Z. *Macromolecules* **2004**, *37*, 181.
(38) Vanden Bout, D. A.; Yip, W.-T.; Hu, D.; Fu, D.-K.; Swager, T. M.; Barbara, P. F. *Science* **1997**, *277*, 1074.
(39) Yu, J.; Song, N. W.; McNeill, J. D.; Barbara, P. F. *Isr. J. Chem.* **2004**, *44*, 127.
(40) Hu, D.; Yu, J.; Padmanaban, G.; Ramakrishnan, S.; Barbara, P. F. *Nano Lett.* **2002**, *2*, 1121.